Spectral Efficiency Comparison Between MC-CDMA Two-Hop Relay Systems With Different Channel Information

Tingting Liu, *Member, IEEE*, and Chenyang Yang, *Senior Member, IEEE*

***Abstract*—The knowledge of channel state information (CSI) is crucial for improving the performance of cooperative communication systems. In multiuser two-hop relay systems, the global CSI between a relay and multiple source-and-destination nodes can be estimated at the relay, and the local CSI between each node and the relay can be estimated at each node. In this paper, we analyze the spectral efficiency of multicarrier code-division multiple-access (MC-CDMA) two-hop relay systems, either with global CSI only at the relay or with local CSI only at every node. We resort to asymptotical analysis with random-matrix theory to derive the average spectral efficiency of decode-and-forward (DF) and amplify-and-forward (AF) two-hop relay systems. We then analyze the impact of spreading sequences, fading channel statistics, and low-complexity transceivers. Analytical and simulation results show that when an orthogonal spreading sequence is used, the relay system with local CSI only at every node is spectrally more efficient than that with global CSI only at the relay. Moreover, an artificially constructed one-tap spreading sequence can achieve a good tradeoff between the performance and the complexity.**

***Index Terms*—Global channel state information (CSI) at the relay, local CSI at each source or destination node, multicarrier code-division multiple access (MC-CDMA), spectral efficiency, two-hop relay.**

I. Introduction

COOPERATIVE transmission has attracted significant research interests in decades, owing to its potential to enhance reliability, coverage, and capacity of wireless systems [1]–[4]. In cooperative communication systems, sharing one relay among multiple source–destination pairs is a cost-efficient way to improve spectral efficiency [2]–[5]. In a multiple-access channel (MAC) phase, the relay receives signals from multiple source nodes. Then, in a broadcast channel (BC) phase, the relay forwards the signals to multiple destination nodes. Such a multiuser two-hop relay system is a building block of various complex relay networks [6], [7].

Manuscript received October 6, 2011; revised January 29, 2012, April 7, 2012, and June 20, 2012; accepted July 1, 2012. Date of publication July 10, 2012; date of current version October 12, 2012. This work was supported in part by the National Natural Science Foundation of China under Grant 61120106002 and Grant 61128002, by the International S&T Cooperation Program of China under Grant 2008DFA12100, and by the China Postdoctoral Science Foundation under Grant 20110490007. The review of this paper was coordinated by Dr. S. Sun.

The authors are with the School of Electronics and Information Engineering, Beihang University, Beijing 100191, China (e-mail: ttliu@ee.buaa.edu.cn; cyyang@buaa.edu.cn).

Color versions of one or more of the figures in this paper are available online at http://ieeexplore.ieee.org.

Digital Object Identifier 10.1109/TVT.2012.2207923

The performance of relay systems largely depends on the knowledge of channel state information (CSI), and different CSI at each node induces different training overhead. In practice, to assist a relay to estimate the global CSI, i.e., all channel coefficients in both source–relay (S–R) links and relay–destination (R–D) links, multiple source and destination nodes need to send mutually orthogonal training symbols. Then, the relay can estimate all the channels from these nodes to itself and obtain the channels from itself to the nodes by exploiting channel reciprocity in time-division duplex (TDD) systems. To assist each source node and each destination node to acquire the local CSI, i.e., the channel coefficients from each source to the relay and those from the relay to each destination, the relay only needs to broadcast one training symbol to the nodes. In a two-hop relay system with K pairs of users, to provide the global CSI for the relay, $2K$ training symbols are required in total, whereas to provide the local CSI for every source and destination nodes, only one training symbol is necessary.

When the global CSI is available at both the relay and all nodes,[1] a jointly optimized S–R–D transceiver provides the best performance in single-user two-hop relay systems [8], [9]. In the multiuser setting, however, due to the large overhead for acquiring the CSI and the high complexity for iteratively computing the transmit and receive vectors at the relay and all nodes [5], [10], such a joint optimization is not desirable for practical systems. This calls for a decoupled transceiver design, which has low overhead and low complexity but with acceptable performance loss.

In this paper, we study TDD multicarrier code-division multiple-access (MC-CDMA) two-hop relay systems. MC-CDMA is able to employ low-complexity frequency-domain transceiver for broad-band systems, which achieves a good tradeoff between reliability and capacity [11]. Specifically, we investigate the performance of the relay systems with different kinds of channel knowledge when decoupled linear transceivers are employed at the relay and each node, which is of practical interest.

We first consider a system where the relay has the global CSI, but the source and destination nodes have no channel information. In the MAC phase, the relay can apply a detector to cancel the multiuser interference (MUI) from multiple source

[1] To differentiate the relay systems with various kinds of channel information, we do not call the relay a node in this paper.

nodes [12]–[14], whereas the source nodes can transmit the signals simply by spreading the signals. In the BC phase, the relay can employ a precoder to avoid the interference to different destination nodes, and each destination node can obtain its desired symbol only by despreading the signal. We then consider a system where the local CSI is available at every source node and every destination node, but the relay has no channel knowledge. In this scenario, each source node can individually exploit the CSI for computing its precoder to avoid the MUI, and each destination node can employ a channel-dependent detector to cancel the MUI. The relay needs to do nothing more than despreading during reception and spreading during transmission. One may expect that a multiuser two-hop relay system where only the relay has the global CSI outperforms a system where only every node has its local CSI. However, it remains unclear what kind of CSI can provide higher spectral efficiency.

To answer this question, we compare the average spectral efficiency of the MC-CDMA two-hop relay systems with only global CSI at the relay and only local CSI at every node. We then analyze the impact of spreading sequences and channel statistics on the spectral efficiency. Both analytical and simulation results show that, in Nakagami-m fading channels, when random spreading sequence is used, the system with the global CSI is spectrally more efficient than the system with the local CSI. When orthogonal spreading sequence is employed, the conclusion is just the opposite. We also analyze the impact of a low-complexity transceiver at each node on the average spectral efficiency.

The remainder of this paper is organized as follows. In Section II, we introduce the signal model and the transmission scheme. We analyze the spectral efficiency of the relay systems with only global CSI at the relay and only local CSI at every node in Sections III and IV, respectively, and compare their performance in Section V. Simulation results are provided in Section VI, and conclusions are drawn in Section VII.

Notations: Bold uppercase and lowercase variables are used to denote matrices and vectors, respectively. Conjugation, transpose, Hermitian transpose, and expectation are represented by $(\cdot)^*$, $(\cdot)^T$, $(\cdot)^H$, and $\mathbb{E}\{\cdot\}$, respectively. The trace of a square matrix is denoted as $\mathrm{tr}\{\cdot\}$, the diagonal matrix is denoted as $\mathrm{diag}\{\cdots\}$, and the norm of vector $\boldsymbol{x}$ is denoted as $\|\boldsymbol{x}\| = \sqrt{\boldsymbol{x}^H\boldsymbol{x}}$.

II. System Description

A. System Models

We consider a MC-CDMA two-hop relay system with M subcarriers, as shown in Fig. 1, where the transmissions from sources $\mathcal{S}_1, \ldots, \mathcal{S}_K$ to destinations $\mathcal{D}_1, \ldots, \mathcal{D}_K$ are assisted by a half-duplex relay $\mathcal{R}$. The load factor is $\beta = K/M$. In the figure, $\boldsymbol{H}_{\mathcal{S}_k} = \mathrm{diag}\{H_{\mathcal{S}_k}^{(1)}, \ldots, H_{\mathcal{S}_k}^{(M)}\}$, and $\boldsymbol{H}_{\mathcal{D}_k} = \mathrm{diag}\{H_{\mathcal{D}_k}^{(1)}, \ldots, H_{\mathcal{D}_k}^{(M)}\}$, whose diagonal elements denote the frequency-domain channel responses from source $\mathcal{S}_k$ to the relay and those from the relay to destination $\mathcal{D}_k$, respectively.

In the following, when both $\boldsymbol{H}_{\mathcal{S}_1}, \ldots, \boldsymbol{H}_{\mathcal{S}_K}$ and $\boldsymbol{H}_{\mathcal{D}_1}, \ldots, \boldsymbol{H}_{\mathcal{D}_K}$ are available at the relay but all the nodes have no channel information, we say that this system has *global CSI at the relay*. When $\boldsymbol{H}_{\mathcal{S}_k}$ is available at source $\mathcal{S}_k$ and $\boldsymbol{H}_{\mathcal{D}_k}$ is known at destination $\mathcal{D}_k$ $(k = 1, \ldots, K)$ but the relay has no channel information, we say that this relay system has *local CSI at every node*.

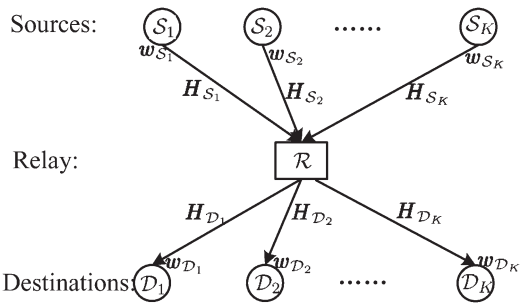

Fig. 1. Multiuser two-hop cooperative network with K source–destination pairs assisted by a single relay.

In the MAC phase, source $\mathcal{S}_k$ uses an M-length frequency-domain transmit vector $\boldsymbol{w}_{\mathcal{S}_k}$ to convey its symbol d_k. The transmit symbols $d_1, \ldots, d_K$ are assumed independent and identically distributed (i.i.d.) random variables satisfying $\mathbb{E}\{d_k\} = 0$ and $\mathbb{E}\{|d_k|^2\} = 1$. The frequency-domain signal received at relay $\mathcal{R}$ is

$$\boldsymbol{y}_{\mathcal{R}} = \sum_{k=1}^{K} \sqrt{\alpha_{\mathcal{S}_k}} \boldsymbol{H}_{\mathcal{S}_k} \boldsymbol{w}_{\mathcal{S}_k} d_k + \boldsymbol{n}_{\mathcal{R}} \tag{1}$$

where $\alpha_{\mathcal{S}_k} = P_{\mathcal{S}} / \boldsymbol{w}_{\mathcal{S}_k}^H \boldsymbol{w}_{\mathcal{S}_k}$ is an amplification factor that meets the transmit power constraint of the kth source, $P_{\mathcal{S}}$ is the maximal transmit power per symbol at the source, $\boldsymbol{n}_{\mathcal{R}}$ is an M-length zero-mean Gaussian noise vector with covariance matrix $\mathbb{E}\{\boldsymbol{n}_{\mathcal{R}} \boldsymbol{n}_{\mathcal{R}}^H\} = \sigma_{\mathcal{R}}^2 \boldsymbol{I}_M$, and $\sigma_{\mathcal{R}}^2$ is the noise variance at the relay.

In the BC phase, the transmit signal of the relay depends on the forwarding strategies. We consider the two most popular strategies: decode-and-forward (DF) and amplify-and-forward (AF).

When employing DF, the relay first uses a receive vector $\boldsymbol{w}_{\mathcal{R}r_k}$ to estimate the kth symbol as

$$\hat{d}_{\mathcal{R}_k} = \boldsymbol{w}_{\mathcal{R}r_k}^H \boldsymbol{y}_{\mathcal{R}} = \sum_{k=1}^{K} \sqrt{\alpha_{\mathcal{S}_k}} \boldsymbol{w}_{\mathcal{R}r_k}^H \boldsymbol{H}_{\mathcal{S}_k} \boldsymbol{w}_{\mathcal{S}_k} d_k + \boldsymbol{w}_{\mathcal{R}r_k}^H \boldsymbol{n}_{\mathcal{R}} \tag{2}$$

then decodes the kth symbol $d_{\mathcal{R}_k}$ from $\hat{d}_{\mathcal{R}_k}$. Next, the relay employs transmit vector $\boldsymbol{w}_{\mathcal{R}t_k}$ to forward $d_{\mathcal{R}_k}$ to the kth destination. The signal to be forwarded at the relay can be expressed as

$$\boldsymbol{x}_{\mathcal{R}}^{\mathrm{DF}} = \sum_{k=1}^{K} \sqrt{\alpha_{\mathcal{R}_k}^{\mathrm{DF}}} \boldsymbol{w}_{\mathcal{R}t_k} d_{\mathcal{R}_k} \tag{3}$$

where $\alpha_{\mathcal{R}_k}^{\mathrm{DF}} = P_{\mathcal{R}} / \boldsymbol{w}_{\mathcal{R}t_k}^H \boldsymbol{w}_{\mathcal{R}t_k}$ is an amplification factor that meets the transmit power constraint, and $P_{\mathcal{R}}$ is the maximal transmit power per symbol at the relay.

When employing AF, the relay uses a linear transceiver $\boldsymbol{w}_{\mathcal{R}_k}$ to directly forward the received signal. The analysis in [12]

indicates that the transceiver at the AF relay can be decoupled into a linear detector in the MAC phase and a linear precoder in the BC phase with no performance loss, i.e., $\boldsymbol{w}_{\mathcal{R}_k} = \boldsymbol{w}_{\mathcal{R}t_k}\boldsymbol{w}_{\mathcal{R}r_k}^H$. As a result, the forwarded signal becomes

$$\boldsymbol{x}_{\mathcal{R}}^{\mathrm{AF}} = \sum_{k=1}^{K} \sqrt{\alpha_{\mathcal{R}_k}^{\mathrm{AF}}}\boldsymbol{w}_{\mathcal{R}t_k}\boldsymbol{w}_{\mathcal{R}r_k}^H\boldsymbol{y}_{\mathcal{R}} \tag{4}$$

where $\alpha_{\mathcal{R}_k}^{\mathrm{AF}} = P_{\mathcal{R}}/\mathrm{tr}\{\boldsymbol{w}_{\mathcal{R}t_k}\boldsymbol{w}_{\mathcal{R}r_k}^H\mathbb{E}\{\boldsymbol{y}_{\mathcal{R}}\boldsymbol{y}_{\mathcal{R}}^H\}\boldsymbol{w}_{\mathcal{R}r_k}^H\boldsymbol{w}_{\mathcal{R}t_k}\}$ is an amplification factor that meets the transmit power constraint at the relay.

The frequency-domain signal received at the kth destination is

$$\boldsymbol{y}_{\mathcal{D}_k} = \boldsymbol{H}_{\mathcal{D}_k}^T\boldsymbol{x}_{\mathcal{R}} + \boldsymbol{n}_{\mathcal{D}_k} \tag{5}$$

where $\boldsymbol{n}_{\mathcal{D}_k}$ is an M-length zero-mean Gaussian noise vector with covariance matrix $\mathbb{E}\{\boldsymbol{n}_{\mathcal{D}_k}\boldsymbol{n}_{\mathcal{D}_k}^H\} = \sigma_{\mathcal{D}}^2\boldsymbol{I}_M$, and $\sigma_{\mathcal{D}}^2$ is the noise variance at the destination.

Finally, destination $\mathcal{D}_k$ employs receive vector $\boldsymbol{w}_{\mathcal{D}_k}$ to estimate its desired symbol, i.e.,

$$\hat{d}_{\mathcal{D}_k} = \boldsymbol{w}_{\mathcal{D}_k}^H\boldsymbol{y}_{\mathcal{D}_k} = \boldsymbol{w}_{\mathcal{D}_k}^H\boldsymbol{H}_{\mathcal{D}_k}^T\boldsymbol{x}_{\mathcal{R}} + \boldsymbol{w}_{\mathcal{D}_k}^H\boldsymbol{n}_{\mathcal{D}_k}. \tag{6}$$

B. Spectral Efficiency

For the DF relay, the performance is limited by the worse link in the two phases [1]; thus, the spectral efficiency is

$$\mathrm{SE}^{\mathrm{DF}} = \frac{1}{2M}\sum_{k=1}^{K}\log\left(1 + \min\{\gamma_{\mathrm{MAC}_k}, \gamma_{\mathrm{BC}_k}\}\right) \tag{7}$$

where the factor 1/2 comes from the fact that the transmission consists of two hops, γ_{MAC_k} and γ_{BC_k} are the signal-to-interference-plus-noise ratio (SINR) in the MAC and BC phases, respectively.

For the AF relay, a key step for deriving the spectral efficiency is to derive the end-to-end SINR in the S–R–D link. Although we can obtain the exact SINR expression following a similar way as in [12], it is too complicated to gain useful insight and analyze further. Instead, we introduce an approximation to simplify the expression and validate the results via simulations later.

It has been shown that, in additive white Gaussian noise (AWGN) channel, the end-to-end SNR is a function of the SNRs in the MAC and BC phases [1]. In this paper, the residual interference plus noise at the outputs of the linear receivers at the relay and destination can be approximated as Gaussian random variables that are independent of each other. Applying the Gaussian approximation, the end-to-end SINR of the AF relay can be approximated as a function of the SINRs in the two phases as in [1], i.e., $\gamma_k = \gamma_{\mathrm{MAC}_k}\gamma_{\mathrm{BC}_k}/(\gamma_{\mathrm{MAC}_k} + \gamma_{\mathrm{BC}_k} + 1)$. Therefore, the spectral efficiency of the AF relay can be approximated as

$$\mathrm{SE}^{\mathrm{AF}} \approx \frac{1}{2M}\sum_{k=1}^{K}\log\left(1 + \frac{\gamma_{\mathrm{MAC}_k}\gamma_{\mathrm{BC}_k}}{\gamma_{\mathrm{MAC}_k} + \gamma_{\mathrm{BC}_k} + 1}\right). \tag{8}$$

III. Global Channel Information at the Relay

Here, we first investigate the average spectral efficiency of the relay system with *global CSI at the relay*.

Without any CSI, source $\mathcal{S}_k$ and destination $\mathcal{D}_k$ can simply employ spreading sequence $\boldsymbol{c}_k$ to transmit and receive the desired symbol d_k, i.e., $\boldsymbol{w}_{\mathcal{S}_k} = \boldsymbol{c}_k$ and $\boldsymbol{w}_{\mathcal{D}_k} = \boldsymbol{c}_k^*$. For simplicity, we assume $\boldsymbol{c}_k^H\boldsymbol{c}_k = 1$.

With global CSI, relay $\mathcal{R}$ can employ an optimal multiuser transceiver. In [12], an egocentric–altruistic (E–A) optimization was investigated for relay systems. It yields a maximal SINR (Max-SINR) detector in the MAC phase and a maximal signal-to-leakage-plus-noise ratio (Max-SLNR) precoder in the BC phase for the relay. Such a transceiver is equivalent to a linear optimal transceiver obtained from minimum-mean-square-error criterion. For analytical tractability, we employ the E–A optimization to design $\boldsymbol{w}_{\mathcal{R}r_k}$ and $\boldsymbol{w}_{\mathcal{R}t_k}$. From [12], we have

$$\boldsymbol{w}_{\mathcal{R}r_k} = \left(\sum_{i=1}^{K}\boldsymbol{H}_{\mathcal{S}_i}\boldsymbol{c}_i\boldsymbol{c}_i^H\boldsymbol{H}_{\mathcal{S}_i}^H + \frac{\sigma_{\mathcal{R}}^2}{P_{\mathcal{S}}}\boldsymbol{I}_M\right)^{-1}\boldsymbol{H}_{\mathcal{S}_k}\boldsymbol{c}_k \tag{9}$$

$$\boldsymbol{w}_{\mathcal{R}t_k} = \left(\sum_{i=1}^{K}\boldsymbol{H}_{\mathcal{D}_i}^*\boldsymbol{c}_i^*\boldsymbol{c}_i^T\boldsymbol{H}_{\mathcal{D}_i}^T + \frac{\sigma_{\mathcal{D}}^2}{P_{\mathcal{R}}}\boldsymbol{I}_M\right)^{-1}\boldsymbol{H}_{\mathcal{D}_k}^*\boldsymbol{c}_k^*. \tag{10}$$

By substituting $\boldsymbol{w}_{\mathcal{S}_k} = \boldsymbol{c}_k$ and (9) into (2), the SINR of the kth symbol in the MAC phase is obtained as

$$\gamma_{\mathrm{MAC}_k}^{G} = \frac{P_{\mathcal{S}}/\sigma_{\mathcal{R}}^2}{\boldsymbol{e}_k^H\left(\bar{\boldsymbol{H}}_{\mathcal{SR}}^H\bar{\boldsymbol{H}}_{\mathcal{SR}} + \sigma_{\mathcal{R}}^2/P_{\mathcal{S}}\boldsymbol{I}_K\right)^{-1}\boldsymbol{e}_k} - 1 \tag{11}$$

where $\bar{\boldsymbol{H}}_{\mathcal{SR}} = [\boldsymbol{H}_{\mathcal{S}_1}\boldsymbol{c}_1, \ldots, \boldsymbol{H}_{\mathcal{S}_K}\boldsymbol{c}_K] \in \mathbb{C}^{M\times K}$ is the equivalent channel matrix in the MAC phase seen at the relay, and $\boldsymbol{e}_k$ is a basis vector, whose kth entry is 1, and all the other entries are 0.

Similarly, substituting $\boldsymbol{w}_{\mathcal{D}_k} = \boldsymbol{c}_k^*$ and (10) into (6), we can obtain the SINR of the kth symbol in the BC phase. However, the obtained SINR expression is too complicated to analyze. Based on the duality between the transmitter and the receiver optimization, as shown in [15], the SINR achieved by precoder $\boldsymbol{w}_{\mathcal{R}t_k}$ in the R–D link can be approximated as the SINR achieved by detector $\boldsymbol{w}_{\mathcal{R}r_k} = \boldsymbol{w}_{\mathcal{R}t_k}^*$ in the D–R link. Therefore, the SINR in the BC phase can be approximated as

$$\gamma_{\mathrm{BC}_k}^{G} \approx \frac{P_{\mathcal{R}}/\sigma_{\mathcal{D}}^2}{\boldsymbol{e}_k^H\left(\bar{\boldsymbol{H}}_{\mathcal{DR}}^T\bar{\boldsymbol{H}}_{\mathcal{DR}}^* + \sigma_{\mathcal{D}}^2/P_{\mathcal{R}}\boldsymbol{I}_K\right)^{-1}\boldsymbol{e}_k} - 1 \tag{12}$$

where $\bar{\boldsymbol{H}}_{\mathcal{DR}} = [\boldsymbol{H}_{\mathcal{D}_1}\boldsymbol{c}_1, \ldots, \boldsymbol{H}_{\mathcal{D}_K}\boldsymbol{c}_K] \in \mathbb{C}^{M\times K}$ is the equivalent channel matrix in the BC phase seen at the relay.

By substituting (11) and (12) into (7) and (8), we can obtain the instantaneous spectral efficiency of the DF and AF systems, respectively. With the probability density function (pdf) of fading channels, we can derive the average spectral efficiency. However, the study in [16] indicates that when the number of user pairs $K > 2$, it is intractable to derive a closed-form expression of the average spectral efficiency.

Fortunately, as $K, M \to \infty$ with $K/M \to \beta$, we can derive a closed-form expression for asymptotic spectral efficiency by

using random-matrix theory. Moreover, the asymptotic spectral efficiency converges in mean square to the average spectral efficiency. As will be shown later, the asymptotic spectral efficiency is quite close to the average spectral efficiency even with finite K and M. In the sequel, we will investigate the asymptotic spectral efficiency.

In random-matrix theory [17], η-transform is an important tool for asymptotic analysis, whose definition is shown as follows for readers' convenience.

Definition 1: The η-transform of a nonnegative definite random matrix $\boldsymbol{V}$ is

$$\eta_{\boldsymbol{V}}(x) \triangleq \mathbb{E}\left\{\frac{1}{1+x\lambda_{\boldsymbol{V}}}\right\} = \int \frac{f_{\boldsymbol{V}}(t)}{1+xt}\,dt \tag{13}$$

where $\lambda_{\boldsymbol{V}}$ is the eigenvalue of $\boldsymbol{V}$, $f_{\boldsymbol{V}}(x)$ is the pdf of $\lambda_{\boldsymbol{V}}$, and x is a nonnegative real number.

From (11), it is not hard to derive the asymptotic SINR in the MAC phase as follows:

$$\begin{aligned}\bar{\gamma}^{G}_{\mathrm{MAC}_k} &= \lim_{K\to\infty} \frac{P_{\mathcal{S}}/\sigma^2_{\mathcal{R}}}{\boldsymbol{e}_k^H\left(\bar{\boldsymbol{H}}^H_{\mathcal{SR}}\bar{\boldsymbol{H}}_{\mathcal{SR}} + \sigma^2_{\mathcal{R}}/P_{\mathcal{S}}\boldsymbol{I}_K\right)^{-1}\boldsymbol{e}_k} - 1 \\ &= \lim_{K\to\infty} \frac{1}{\frac{1}{K}\mathrm{tr}\left\{\left(P_{\mathcal{S}}/\sigma^2_{\mathcal{R}}\bar{\boldsymbol{H}}^H_{\mathcal{SR}}\bar{\boldsymbol{H}}_{\mathcal{SR}} + \boldsymbol{I}_K\right)^{-1}\right\}} - 1 \\ &= \eta^{-1}_{\bar{\boldsymbol{H}}^H_{\mathcal{SR}}\bar{\boldsymbol{H}}_{\mathcal{SR}}}\left(P_{\mathcal{S}}/\sigma^2_{\mathcal{R}}\right) - 1. \end{aligned} \tag{14}$$

To simplify the analysis, we assume that the channel coefficient at each subcarrier is a zero-mean random variable with unit variance, and the channel coefficients among the subcarriers are independent of each other. We will show in simulations later that the obtained conclusion is still valid when adjacent subcarriers are correlated. Furthermore, we assume that the channels among multiple users are mutually independent. As a result, no matter what kind of spreading sequences are used, all the elements of the equivalent channel matrix $\bar{\boldsymbol{H}}_{\mathcal{SR}}$ are i.i.d. random variables. Since the frequency-domain channel response $H^{(m)}_{\mathcal{S}_k}$ is zero mean and with unit variance and the spreading sequence satisfies $\boldsymbol{c}_k^H\boldsymbol{c}_k = 1$, the elements of $\bar{\boldsymbol{H}}_{\mathcal{SR}}$ are zero mean and with variance $1/M$. Then, according to the Marcenko–Pastur law [17], as $K, M \to \infty$ with $K/M \to \beta$, the empirical distribution of the eigenvalues of equivalent channel correlation matrix $\bar{\boldsymbol{H}}^H_{\mathcal{SR}}\bar{\boldsymbol{H}}_{\mathcal{SR}}$ converges with a probability of 1 to a distribution whose η-transform satisfies

$$\eta_{\bar{\boldsymbol{H}}^H_{\mathcal{SR}}\bar{\boldsymbol{H}}_{\mathcal{SR}}}(x) = 1 - \frac{\mathcal{F}(x,\beta)}{4\beta x} \tag{15}$$

where

$$\mathcal{F}(x,z) \triangleq \left(\sqrt{1+x(1+\sqrt{z})^2} - \sqrt{1+x(1-\sqrt{z})^2}\right)^2.$$

By substituting (15) into (14), the asymptotic SINR can be derived as

$$\bar{\gamma}^{G}_{\mathrm{MAC}_k} = \frac{P_{\mathcal{S}}}{\sigma^2_{\mathcal{R}}} - \frac{1}{4}\mathcal{F}\left(\frac{P_{\mathcal{S}}}{\sigma^2_{\mathcal{R}}}, \beta\right). \tag{16}$$

The analysis in [17] shows that, for large-scale systems, where $K, M \to \infty$, the interference power from user i to user k equals to the leakage power from user k to user i. Consequently, the SLNR equals to the SINR. This implies that, in the asymptotic region, the relay transceiver consisting of the Max-SLNR precoder and the Max-SINR detector achieves the same performance as an optimal relay transceiver designed under the Max-SINR criterion.

It is not difficult to show that the right-hand side of (12) is the exact SLNR expression in the BC phase. Based on the equivalency between the SINR and the SLNR in the asymptotic region, the asymptotic SINR in the BC phase can be derived as

$$\bar{\gamma}^{G}_{\mathrm{BC}_k} = \frac{P_{\mathcal{R}}}{\sigma^2_{\mathcal{D}}} - \frac{1}{4}\mathcal{F}\left(\frac{P_{\mathcal{R}}}{\sigma^2_{\mathcal{D}}}, \beta\right). \tag{17}$$

By substituting (16) and (17) into (7) and (8), respectively, we can obtain the asymptotic spectral efficiency of the DF and AF relay systems with global CSI at the relay. It shows that the asymptotic performance depends on the SNRs $P_{\mathcal{S}}/\sigma^2_{\mathcal{R}}$ and $P_{\mathcal{R}}/\sigma^2_{\mathcal{D}}$, as well as the asymptotic load factor β, but does not depend on the characteristics of the spreading sequences and fading channels.

IV. Local Channel Information at Sources and Destinations

When all the source and destination nodes have the local CSI, they can design the channel-dependent precoders and detectors. With no CSI, the relay employs a spreading sequence to receive and forward the kth symbol, i.e., $\boldsymbol{w}_{\mathcal{R}r_k} = \boldsymbol{c}_k$ and $\boldsymbol{w}_{\mathcal{R}t_k} = \boldsymbol{c}_k^*$.

For a fair comparison, the same criteria are considered here as we optimize the relay transceiver for the system with global CSI at the relay. The Max-SLNR precoder at the source is obtained as

$$\boldsymbol{w}_{\mathcal{S}_k} = \left(\sum_{i=1}^{K}\boldsymbol{H}^H_{\mathcal{S}_k}\boldsymbol{c}_i\boldsymbol{c}_i^H\boldsymbol{H}_{\mathcal{S}_k} + \frac{\sigma^2_{\mathcal{R}}}{P_{\mathcal{S}}}\boldsymbol{I}_M\right)^{-1}\boldsymbol{H}^H_{\mathcal{S}_k}\boldsymbol{c}_k \tag{18}$$

and the Max-SINR detector at the destination is

$$\boldsymbol{w}_{\mathcal{D}_k} = \left(\sum_{i=1}^{K}\boldsymbol{H}^T_{\mathcal{D}_k}\boldsymbol{c}_i^*\boldsymbol{c}_i^T\boldsymbol{H}_{\mathcal{D}_k} + \frac{\sigma^2_{\mathcal{D}}}{P_{\mathcal{R}}}\boldsymbol{I}_M\right)^{-1}\boldsymbol{H}^T_{\mathcal{D}_k}\boldsymbol{c}_k^*. \tag{19}$$

By substituting (19) into (6), the SINR in the BC phase is derived as

$$\gamma^{L}_{\mathrm{BC}_k} = \frac{P_{\mathcal{R}}/\sigma^2_{\mathcal{D}}}{\boldsymbol{e}_k^H\left(\boldsymbol{C}^T\boldsymbol{\Delta}_{\mathcal{D}_k}\boldsymbol{C}^* + \sigma^2_{\mathcal{D}}/P_{\mathcal{R}}\boldsymbol{I}_K\right)^{-1}\boldsymbol{e}_k} - 1 \tag{20}$$

where $\boldsymbol{C} = [\boldsymbol{c}_1, \ldots, \boldsymbol{c}_K]$ is the spreading sequence matrix, $\boldsymbol{\Delta}_{\mathcal{D}_k} = \boldsymbol{H}_{\mathcal{D}_k}\boldsymbol{H}^H_{\mathcal{D}_k} = \mathrm{diag}\{|H^{(1)}_{\mathcal{D}_k}|^2, \ldots, |H^{(M)}_{\mathcal{D}_k}|^2\}$, whose diagonal elements denote the channel power values of the M subcarriers in the link from relay $\mathcal{R}$ to destination $\mathcal{D}_k$.

The SINR in the MAC phase can be similarly obtained by substituting (18) into (2), which is, unfortunately, too complicated to analyze. Again, using the duality between the

transmitter and the receiver optimization [15], the SINR can be approximated as

$$\gamma_{\mathrm{MAC}_k}^{L} \approx \frac{P_{\mathcal{S}}/\sigma_{\mathcal{R}}^2}{\boldsymbol{e}_k^H \left(\boldsymbol{C}^H \boldsymbol{\Delta}_{\mathcal{S}_k} \boldsymbol{C} + \sigma_{\mathcal{R}}^2/P_{\mathcal{S}} \boldsymbol{I}_K\right)^{-1} \boldsymbol{e}_k} - 1 \quad (21)$$

where $\boldsymbol{\Delta}_{\mathcal{S}_k} = \boldsymbol{H}_{\mathcal{S}_k}\boldsymbol{H}_{\mathcal{S}_k}^H = \mathrm{diag}\{|H_{\mathcal{S}_k}^{(1)}|^2, \ldots, |H_{\mathcal{S}_k}^{(M)}|^2\}$, whose diagonal elements denote the channel power values in the link from source $\mathcal{S}_k$ to relay $\mathcal{R}$.

It is not hard to derive the asymptotic SINR in the MAC phase as follows:

$$\begin{aligned}\bar{\gamma}_{\mathrm{MAC}_k}^{L} &= \lim_{K\to\infty} \frac{1}{\frac{1}{K}\mathrm{tr}\left\{\left(\frac{P_{\mathcal{S}}}{\sigma_{\mathcal{R}}^2}\boldsymbol{C}^H\boldsymbol{\Delta}_{\mathcal{S}_k}\boldsymbol{C} + \boldsymbol{I}_K\right)^{-1}\right\}} - 1 \\ &= \frac{1}{\eta_{\boldsymbol{C}^H\boldsymbol{\Delta}_{\mathcal{S}_k}\boldsymbol{C}}\left(P_{\mathcal{S}}/\sigma_{\mathcal{R}}^2\right)} - 1. \end{aligned} \quad (22)$$

In addition, owing to the fact that $\mathrm{tr}\{\boldsymbol{AB}\} = \mathrm{tr}\{\boldsymbol{BA}\}$, the asymptotic SINR in (22) can be rewritten as

$$\begin{aligned}\bar{\gamma}_{\mathrm{MAC}_k}^{L} &= \lim_{K\to\infty} \frac{1}{\frac{1}{K}\mathrm{tr}\left\{\left(\frac{P_{\mathcal{S}}}{\sigma_{\mathcal{R}}^2}\boldsymbol{\Delta}_{\mathcal{S}_k}\boldsymbol{C}\boldsymbol{C}^H + \boldsymbol{I}_M\right)^{-1}\right\} - \frac{M-K}{K}} - 1 \\ &= \frac{\beta}{\eta_{\boldsymbol{\Delta}_{\mathcal{S}_k}\boldsymbol{C}\boldsymbol{C}^H}\left(P_{\mathcal{S}}/\sigma_{\mathcal{R}}^2\right) + \beta - 1} - 1. \end{aligned} \quad (23)$$

When the entries of $M \times K$ spreading sequence matrix $\boldsymbol{C}$ are i.i.d. complex random variables with zero mean and variance $1/M$, we call $\boldsymbol{c}_1, \ldots, \boldsymbol{c}_K$ as *random spreading sequences*. In this case, if the equivalent channel correlation matrix $\boldsymbol{\Delta}_{\mathcal{S}_k}$ is a Hermitian random matrix independent of $\boldsymbol{C}$, it is shown in [17, Th. 2.42] that, as $K, M \to \infty$ with $K/M \to \beta$, the empirical distribution of the eigenvalues of $\boldsymbol{\Delta}_{\mathcal{S}_k}\boldsymbol{C}\boldsymbol{C}^H$ converges with a probability of 1 to a distribution whose η-transform satisfies

$$\eta_{\boldsymbol{\Delta}_{\mathcal{S}_k}\boldsymbol{C}\boldsymbol{C}^H}(x) = \eta_{\boldsymbol{\Delta}_{\mathcal{S}_k}}\left(x\left(\eta_{\boldsymbol{\Delta}_{\mathcal{S}_k}\boldsymbol{C}\boldsymbol{C}^H}(x) + \beta - 1\right)\right) \quad (24)$$

where $\eta_{\boldsymbol{\Delta}_{\mathcal{S}_k}}$ is the η-transform of $\boldsymbol{\Delta}_{\mathcal{S}_k}$.

When $\boldsymbol{C}$ is a random matrix uniformly distributed over the manifold of $M \times K$ complex matrices such that $\boldsymbol{C}^H\boldsymbol{C} = \boldsymbol{I}$, we call $\boldsymbol{c}_1, \ldots, \boldsymbol{c}_K$ as *orthogonal spreading sequences*. In this case, if $\boldsymbol{\Delta}_{\mathcal{S}_k}$ is still the random matrix independent of $\boldsymbol{C}$, it is shown in [17, Ex. 2.51] that, as $K, M \to \infty$ with $K/M \to \beta$, the empirical distribution of the eigenvalues of $\boldsymbol{\Delta}_{\mathcal{S}_k}\boldsymbol{C}\boldsymbol{C}^H$ converges with a probability of 1 to a distribution whose η-transform satisfies

$$\eta_{\boldsymbol{\Delta}_{\mathcal{S}_k}\boldsymbol{C}\boldsymbol{C}^H}(x) = \eta_{\boldsymbol{\Delta}_{\mathcal{S}_k}}\left(x\frac{\eta_{\boldsymbol{\Delta}_{\mathcal{S}_k}\boldsymbol{C}\boldsymbol{C}^H}(x) + \beta - 1}{\eta_{\boldsymbol{\Delta}_{\mathcal{S}_k}\boldsymbol{C}\boldsymbol{C}^H}(x)}\right). \quad (25)$$

From (23), the η-transform of $\boldsymbol{\Delta}_{\mathcal{S}_k}\boldsymbol{C}\boldsymbol{C}^H$ can also be expressed as a function of the asymptotic SINR, i.e.,

$$\eta_{\boldsymbol{\Delta}_{\mathcal{S}_k}\boldsymbol{C}\boldsymbol{C}^H}\left(\frac{P_{\mathcal{S}}}{\sigma_{\mathcal{R}}^2}\right) = \frac{\beta}{\bar{\gamma}_{\mathrm{MAC}_k}^{L} + 1} - \beta + 1. \quad (26)$$

By substituting (26) into (24) and after some regular manipulations, the asymptotic SINR with the random spreading sequence can be shown to satisfy the following:

$$\beta\frac{\bar{\gamma}_{\mathrm{MAC}_k}^{L-\mathrm{Rand}}}{\bar{\gamma}_{\mathrm{MAC}_k}^{L-\mathrm{Rand}} + 1} = 1 - \eta_{\boldsymbol{\Delta}_{\mathcal{S}_k}}\left(\frac{P_{\mathcal{S}}}{\sigma_{\mathcal{R}}^2}\frac{\beta}{\bar{\gamma}_{\mathrm{MAC}_k}^{L-\mathrm{Rand}} + 1}\right). \quad (27)$$

Similarly, substituting (26) into (25), the asymptotic SINR with the orthogonal spreading sequence can be shown as a solution of the following:

$$\beta\frac{\bar{\gamma}_{\mathrm{MAC}_k}^{L-\mathrm{Orth}}}{\bar{\gamma}_{\mathrm{MAC}_k}^{L-\mathrm{Orth}} + 1} = 1 - \eta_{\boldsymbol{\Delta}_{\mathcal{S}_k}}\left(\frac{P_{\mathcal{S}}}{\sigma_{\mathcal{R}}^2}\frac{\beta}{(1-\beta)\bar{\gamma}_{\mathrm{MAC}_k}^{L-\mathrm{Orth}} + 1}\right). \quad (28)$$

Equations (27) and (28) can be expressed in a unified form as

$$\beta\frac{\bar{\gamma}_{\mathrm{MAC}_k}^{L}}{\bar{\gamma}_{\mathrm{MAC}_k}^{L} + 1} + \eta_{\boldsymbol{\Delta}_{\mathcal{S}_k}}\left(\frac{P_{\mathcal{S}}}{\sigma_{\mathcal{R}}^2}\frac{\beta}{\phi\bar{\gamma}_{\mathrm{MAC}_k}^{L} + 1}\right) - 1 = 0 \quad (29)$$

where $\phi = 1$ denotes the SINR using the random spreading sequence, and $\phi = 1 - \beta$ represents the SINR using the orthogonal spreading sequence.

From (29), we can see that using different spreading sequences leads to different asymptotic SINR for the relay system with local CSI at every node. Moreover, as will be shown soon, the asymptotic SINR depends on the statistics of fading channels as well. These results are very different from those for the system with global CSI at the relay, which is immune to these factors. In the following, we will further study the impact of the spreading sequences and fading channels by taking the SINR in the MAC phase as an example. We will also analyze the impact of the low-complexity transceiver, which is of practical importance.

A. Impact of Spreading Sequences

It is hard to analyze the impact of the spreading sequences by directly comparing (27) and (28) because they are not closed-form expressions of the SINR. In the following, we simplify the SINR expressions by introducing approximations.

To obtain accurate approximations for different SNR levels, we first analyze how the SINR varies with the SNR. In Appendix A, we know that $\partial\bar{\gamma}_{\mathrm{MAC}_k}^{L}/\partial(P_{\mathcal{S}}/\sigma_{\mathcal{R}}^2) > 0$. This shows that the asymptotic SINR is an increasing function of the SNR $P_{\mathcal{S}}/\sigma_{\mathcal{R}}^2$. Then, at a high SNR level, we can approximate $\bar{\gamma}_{\mathrm{MAC}_k}^{L} + 1 \approx \bar{\gamma}_{\mathrm{MAC}_k}^{L}, \forall\beta < 1$. Applying the approximation to (27) and (28), the SINR using the random spreading sequence can be expressed as

$$\bar{\gamma}_{\mathrm{MAC}_k}^{L-\mathrm{Rand}} \approx \frac{P_{\mathcal{S}}}{\sigma_{\mathcal{R}}^2}\frac{\beta}{\varphi_{\boldsymbol{\Delta}_{\mathcal{S}_k}}(1-\beta)} \qquad \forall\beta < 1 \quad (30)$$

while that using the orthogonal spreading sequence becomes

$$\bar{\gamma}_{\mathrm{MAC}_k}^{L-\mathrm{Orth}} \approx \frac{P_{\mathcal{S}}}{\sigma_{\mathcal{R}}^2}\frac{\beta}{(1-\beta)\varphi_{\boldsymbol{\Delta}_{\mathcal{S}_k}}(1-\beta)} \qquad \forall\beta < 1 \quad (31)$$

where $\varphi_{\boldsymbol{\Delta}_{\mathcal{S}_k}}(x)$ is the inverse function of $\eta_{\boldsymbol{\Delta}_{\mathcal{S}_k}}(x)$.

Dividing (31) by (30), we have

$$\frac{\bar{\gamma}_{\mathrm{MAC}_k}^{L-\mathrm{Orth}}}{\bar{\gamma}_{\mathrm{MAC}_k}^{L-\mathrm{Rand}}} = \frac{1}{1-\beta} \qquad \forall \beta < 1. \tag{32}$$

It reflects the SINR gain of the orthogonal spreading sequence over the random spreading sequence.

We can see from (32) that in the high SNR region, the SINR gain depends on the asymptotic load factor but is independent of the characteristic of fading channels. When β $(0 < \beta < 1)$ increases, the SINR gain monotonously increases. This suggests that when the local CSI is available for every source and destination node and the system is underloaded, the advantage of the orthogonal spreading sequence over the random spreading sequence becomes increasingly noticeable as β grows. For any fading channel, the SINR gain never vanishes and always remains a constant.

B. Impact of Fading Channels

Now, we analyze the impact of fading channels.

Theorem 1: Consider two fading channels A and B. Let $\eta_{\mathbf{\Delta}_A}(x)$ and $\eta_{\mathbf{\Delta}_B}(x)$ denote the η-transform of their channel correlation matrices $\mathbf{\Delta}_A^L$ and $\mathbf{\Delta}_B^L$, and $\bar{\gamma}_A^L$ and $\bar{\gamma}_B^L$ be the asymptotic SINRs of the relay system with local CSI at every node in channels A and B, respectively. When $\eta_{\mathbf{\Delta}_A}(x) \geq \eta_{\mathbf{\Delta}_B}(x)$, we have $\bar{\gamma}_A^L \leq \bar{\gamma}_B^L$.

Proof: See Appendix B. ■

Theorem 1 suggests that the asymptotic SINR of the relay system with local CSI at every node monotonically decreases with the η-transform of channel power response. This result is useful for comparing the asymptotic SINRs in different fading channels, with which the closed-form expressions of the SINRs are no longer necessary.

Remark 1: According to Jensen's inequality, from (13), we can derive the lower bound of the η-transform, i.e.,

$$\eta_{\mathbf{\Delta}_{\mathcal{S}_k}}(x) = \mathbb{E}\left\{\frac{1}{1+x\lambda_{\mathbf{\Delta}_{\mathcal{S}_k}}}\right\} \geq \frac{1}{1+x\mathbb{E}\{\lambda_{\mathbf{\Delta}_{\mathcal{S}_k}}\}} = 1/(1+x). \tag{33}$$

Hence, we know that the maximal SINR is achieved when $\eta_{\mathbf{\Delta}_{\mathcal{S}_k}} = 1/(1+x)$. In the AWGN channel, we have $\mathbf{\Delta}_{\mathcal{S}_k} = \boldsymbol{I}$ and $\eta_{\mathbf{\Delta}_{\mathcal{S}_k}}(x) = 1/(1+x)$. Therefore, we can conclude that, in the AWGN channel, the relay system with local CSI at every node can achieve the maximal SINR.

Corollary 1: The upper bounds of $\bar{\gamma}_{\mathrm{MAC}_k}^{L-\mathrm{Rand}}$ and $\bar{\gamma}_{\mathrm{MAC}_k}^{L-\mathrm{Orth}}$ are, respectively, as follows:

$$\bar{\gamma}_{\mathrm{MAC}_k}^{L-\mathrm{Rand}} \leq \frac{P_{\mathcal{S}}}{\sigma_{\mathcal{R}}^2} - \frac{1}{4}\mathcal{F}\left(\frac{P_{\mathcal{S}}}{\sigma_{\mathcal{R}}^2}, \beta\right) \tag{34}$$

$$\bar{\gamma}_{\mathrm{MAC}_k}^{L-\mathrm{Orth}} \leq \frac{P_{\mathcal{S}}}{\sigma_{\mathcal{R}}^2}. \tag{35}$$

Proof: See Appendix C. ■

Corollary 2: In Nakagami-m fading channels, the asymptotic SINR of the relay system with local CSI at each every node is an increasing function of m.

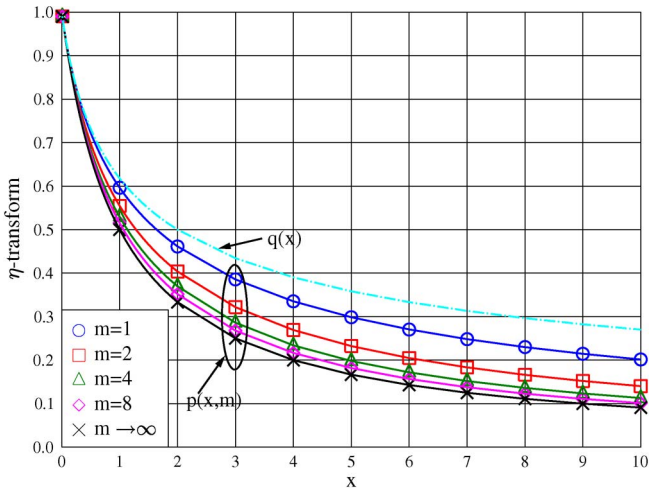

Fig. 2. Comparison of η-transform functions. $p(x,m)$ is obtained from (37), which is $\eta_{\mathbf{\Delta}_{\mathcal{S}_k}}(x)$ in Nakagami-m fading channels. $q(x)$ is obtained from (50).

According to Theorem 1, we can analyze the monotonicity of the asymptotic SINR with m by comparing the values of $\eta_{\mathbf{\Delta}_{\mathcal{S}_k}}(x)$ in Nakagami-m fading channels with different m. To derive $\eta_{\mathbf{\Delta}_{\mathcal{S}_k}}(x)$, we need the pdf of $\mathbf{\Delta}_{\mathcal{S}_k}$ in Nakagami-m channels, which is [18]

$$f_{\mathbf{\Delta}_{\mathcal{S}_k}}(x) = \frac{m^m}{\Gamma(m)} x^{m-1}\exp(-mx) \tag{36}$$

where $\Gamma(x) \triangleq \int_0^\infty e^{-x}x^{x-1}dt$ is the gamma function.

By substituting (36) into (13) and applying [19, eq. (3.382.4)], we obtain

$$\eta_{\mathbf{\Delta}_{\mathcal{S}_k}}(x) = p\,(x,m) \tag{37}$$

where

$$p(x,m) \triangleq \left(\frac{m}{x}\right)^m \exp\left(\frac{m}{x}\right)\Gamma\left(1-m, \frac{m}{x}\right)$$

and $\Gamma(a,x) \triangleq \int_x^\infty e^{-x}x^{a-1}dt$ is the incomplete gamma function.

In Fig. 2, we plot $p(x,m)$ with different m. It is shown that for an arbitrary x, when m increases, the value of $p(x,m)$ monotonically decreases. From Theorem 1, we know that the asymptotic SINR is an increasing function of m.

The Nakagami-m fading channel is able to reflect different communication environments by using different values of parameter m. For instance, it becomes a Rayleigh fading channel when $m = 1$ and converges to an AWGN channel when $m \to \infty$ [20]. As m increases, the amount of fading of the Nakagami-m channels reduces, i.e., the fluctuation of channel power reduces. Therefore, Corollary 2 indicates that a less fluctuated channel attributes to a higher SINR.

C. Impact of The Low-Complexity Transceiver

With only global CSI at the relay, the precoder at each source and the detector at each destination have low complexity, but

the transceiver at the relay is complicated. From (9) and (10), we can see that the complexity of the relay is on the order of $\mathcal{O}(M^3)$ due to an inversion operation of an $M \times M$ matrix. In contrast, only with local CSI at every node, the transceiver of the relay becomes simple, but the precoder at each source and the detector at each destination become complicated, which are on the order of $\mathcal{O}(M^3)$, as shown in (18) and (19). In practice, the processing abilities of the source and destination nodes are usually limited, which impose strict requirement on their complexity. Fortunately, it has been shown in [21] that the complexity of the source and destination nodes could be reduced by judiciously selecting spreading sequences. To see this, we take the precoder at the source as an example.

Let us construct the $M \times K$ spreading sequence matrix $\boldsymbol{C}$ by a $K \times K$ unitary matrix $\boldsymbol{U}$ and an $M \times K$ matrix $\boldsymbol{P}$, i.e.,

$$\boldsymbol{C} = \boldsymbol{P}\boldsymbol{U}. \tag{38}$$

Then, the transmit vector of source $\mathcal{S}_k$ can be expressed as

$$\begin{aligned}\boldsymbol{w}_{\mathcal{S}_k} &= \left(\boldsymbol{H}_{\mathcal{S}_k}^H \boldsymbol{C}\boldsymbol{C}^H \boldsymbol{H}_{\mathcal{S}_k} + \sigma_{\mathcal{R}}^2/P_{\mathcal{S}}\boldsymbol{I}_M\right)^{-1} \boldsymbol{H}_{\mathcal{S}_k}^H \boldsymbol{c}_k \\ &= \boldsymbol{H}_{\mathcal{S}_k}^H \boldsymbol{C}\left(\boldsymbol{C}^H \boldsymbol{\Delta}_{\mathcal{S}_k}\boldsymbol{C} + \sigma_{\mathcal{R}}^2/P_{\mathcal{S}}\boldsymbol{I}_K\right)^{-1} \boldsymbol{e}_k \\ &= \boldsymbol{H}_{\mathcal{S}_k}^H \boldsymbol{P}\left(\boldsymbol{\Pi}_{\mathcal{S}_k} + \sigma_{\mathcal{R}}^2/P_{\mathcal{S}}\boldsymbol{I}_K\right)^{-1} \boldsymbol{U}\boldsymbol{e}_k \end{aligned} \tag{39}$$

where $\boldsymbol{\Pi}_{\mathcal{S}_k} = \boldsymbol{P}^H \boldsymbol{\Delta}_{\mathcal{S}_k}\boldsymbol{P}$.

When the number of nonzero elements in each row of $\boldsymbol{P}$ does not exceed 1, i.e., the elements of the spreading matrix $\boldsymbol{P}$ satisfy

$$P_{l,j}P_{l,i} = 0 \qquad \forall j \neq i \tag{40}$$

the (i,j) element of $\boldsymbol{\Pi}_{\mathcal{S}_k}$ becomes

$$\sum_{l=1}^{M} P_{l,i}P_{l,j}\left|H_{\mathcal{S}_k}^{(l)}\right|^2 = 0 \qquad \forall i \neq j \tag{41}$$

which holds for arbitrary $|H_{\mathcal{S}_k}^{(1)}|^2, \ldots, |H_{\mathcal{S}_k}^{(M)}|^2$.

This way, $\boldsymbol{\Pi}_{\mathcal{S}_k}$ becomes a diagonal matrix, and (39) is reduced to a one-tap frequency-domain precoder. Its complexity is on the order of $\mathcal{O}(K)$, owing to K scalar divisions. We call such an artificially constructed spreading sequence as a one-tap spreading sequence. Since the performance of the relay system with local CSI at every node depends on the spreading sequence, in the sequel, we analyze the performance of the relay system with the one-tap spreading sequence.

To derive the asymptotic SINR, we need to analyze the eigenvalue of $\boldsymbol{C}^H \boldsymbol{\Delta}_{\mathcal{S}_k}\boldsymbol{C}$. Since $\boldsymbol{U}$ is a unitary matrix and $\boldsymbol{\Pi}_{\mathcal{S}_k}$ is a diagonal matrix, $\boldsymbol{C}^H \boldsymbol{\Delta}_{\mathcal{S}_k}\boldsymbol{C} = \boldsymbol{U}^H \boldsymbol{\Pi}_{\mathcal{S}_k}\boldsymbol{U}$ is an eigendecomposition, i.e., $\boldsymbol{\Pi}_{\mathcal{S}_k}$ is the eigenvalue matrix of $\boldsymbol{C}^H \boldsymbol{\Delta}_{\mathcal{S}_k}\boldsymbol{C}$. Hence, the eigenvalues of $\boldsymbol{C}^H \boldsymbol{\Delta}_{\mathcal{S}_k}\boldsymbol{C}$ are

$$\Pi_{\mathcal{S}_k}^{(j)} = \sum_{l=1}^{M} |P_{l,j}|^2 \left|H_{\mathcal{S}_k}^{(l)}\right|^2, \qquad j = 1, \ldots, K. \tag{42}$$

From (42), we can observe that the number of the nonzero elements in each column of $\boldsymbol{P}$, the indexes of these elements, and the weighting coefficients can reflect how many and which subcarriers should be combined, as well as how to combine them.

Based on Corollary 2, we know that when the fluctuation of the channel power is reduced, the SINR will be improved. Analogously, we can show that a less fluctuation of the diagonal elements in $\boldsymbol{\Pi}_{\mathcal{S}_k}$ leads to a higher SINR. To reduce the fluctuation of $\Pi_{\mathcal{S}_k}^{(j)}$, the optimal spreading matrix should be designed in the following manner: Let $\Pi_{\mathcal{S}_k}^{(j)}$ have a form to combine maximal number of subcarriers with maximal spacing and with equal gain weighting. When M is divisible by K, the optimal form of $\Pi_{\mathcal{S}_k}^{(j)}$ can combine M/K subcarriers with an interval of K subcarriers; then, $\Pi_{\mathcal{S}_k}^{(j)} = K/M \sum_{n=0}^{M/K-1} |H_{\mathcal{S}_k}^{(nK+j)}|^2$. In general cases, the optimal form of $\Pi_{\mathcal{S}_k}^{(j)}$ becomes

$$\Pi_{\mathcal{S}_k}^{(j)} = \begin{cases} \frac{1}{N+1}\sum_{n=0}^{N}\left|H_{\mathcal{S}_k}^{(nK+j)}\right|^2, & j \in [1, M-KN] \\ \frac{1}{N}\sum_{n=0}^{N-1}\left|H_{\mathcal{S}_k}^{(nK+j)}\right|^2, & j \in (M-KN, K] \end{cases} \tag{43}$$

where $N = \lfloor M/K \rfloor$.

When an equivalent channel is combined from L i.i.d. channel coefficients in Nakagami-m fading channels whose shape parameter is m, the equivalent channel is subject to another Nakagami-m distribution whose shape parameter is mL [18]. Consequently, from (36) and (43), it is not difficult to derive the pdf of $\Pi_{\mathcal{S}_k}^{(j)}$ as

$$\begin{aligned} f_{\Pi_{\mathcal{S}_k}}(x) = \alpha\frac{m_1^{m_1}}{\Gamma(m_1)}x^{m_1-1}\exp(-m_1 x) \\ +(1-\alpha)\frac{m_2^{m_2}}{\Gamma(m_2)}x^{m_2-1}\exp(-m_2 x) \end{aligned} \tag{44}$$

where $m_1 = m(N+1)$, $m_2 = mN$, and $\alpha = M/K - N$.

By substituting (44) into (13), we have

$$\eta_{\boldsymbol{C}^H\boldsymbol{\Delta}_{\mathcal{S}_k}\boldsymbol{C}}(x) = \alpha p(x, m_1) + (1-\alpha)p(x, m_2) \tag{45}$$

where $p(x,m)$ was defined in (37).

By substituting (45) into (22), the asymptotic SINR provided by the one-tap spreading sequence can be derived as

$$\bar{\gamma}_{\mathrm{MAC}_k}^{L-\mathrm{Onetap}} = \frac{1}{\alpha p\left(\frac{P_{\mathcal{S}}}{\sigma_{\mathcal{R}}^2}, m_1\right) + (1-\alpha)p\left(\frac{P_{\mathcal{S}}}{\sigma_{\mathcal{R}}^2}, m_2\right)} - 1. \tag{46}$$

Applying $\lim_{m\to\infty} p(x,m) = 1/(x+1)$ to (46), we can obtain an upper bound of the SINR, which is

$$\bar{\gamma}_{\mathrm{MAC}_k}^{L-\mathrm{Onetap}} \leq \frac{P_{\mathcal{S}}}{\sigma_{\mathcal{R}}^2}. \tag{47}$$

By comparing with (35), we can see that the orthogonal spreading sequence and the one-tap spreading sequence achieve the same performance bound. However, the forthcoming numerical results will show that the constructed spreading sequence is slightly inferior to the orthogonal spreading sequence. However, as m increases, the performance gap will vanish. This means that the one-tap spreading sequence achieves a good tradeoff between complexity and performance because

it significantly reduces the complexity but only suffers from minor performance loss.

V. Global Channel State Information Versus Local Channel State Information

Based on the aforementioned analytical results, we are able to compare the performance of the relay system with global CSI at the relay and that with local CSI at every node.

Considering that the asymptotic SINR of the system with local CSI depends on the spreading sequences, we compare the performance of the two systems when the random and orthogonal spreading sequences are employed. Again, we take the SINR in the MAC phase as an example. The results in the BC phase are similar and thus are omitted.

A. Random Spreading Sequence

When the random spreading sequence is considered, by comparing (16) with (34), we have

$$\bar{\gamma}_{\mathrm{MAC}_k}^{L-\mathrm{Rand}} \leq \bar{\gamma}_{\mathrm{MAC}_k}^{G}. \tag{48}$$

That is, the system with global CSI at the relay is spectrally more efficient than that with local CSI at every node.

B. Orthogonal Spreading Sequence

When the orthogonal spreading sequence is used, it is difficult to compare the performance of the systems with different CSI by simply comparing (16) and (28). Theorem 1 indicates that we can compare the corresponding $\eta_{\boldsymbol{\Delta}_{\mathcal{S}_k}}$ instead. For the relay system with global CSI at the relay, its η-transform of an equivalent channel correlation matrix is $\eta_{\bar{\boldsymbol{H}}_{\mathcal{SR}}^H \bar{\boldsymbol{H}}_{\mathcal{SR}}}(x)$, as shown in (15). If we can find a channel whose channel correlation matrix $\tilde{\boldsymbol{\Delta}}_{\mathcal{S}_k}$ satisfies $\eta_{\tilde{\boldsymbol{\Delta}}_{\mathcal{S}_k}\boldsymbol{C}\boldsymbol{C}^H}(x) = \eta_{\bar{\boldsymbol{H}}_{\mathcal{SR}}^H \bar{\boldsymbol{H}}_{\mathcal{SR}}}(x)$, the asymptotic SINR of the relay system with global CSI at the relay is equal to that of the system with local CSI at every node.

Therefore, we can indirectly compare the performance of the two systems with different CSI by comparing $\eta_{\boldsymbol{\Delta}_{\mathcal{S}_k}}(x)$ and $\eta_{\tilde{\boldsymbol{\Delta}}_{\mathcal{S}_k}}(x)$.

By substituting $\eta_{\tilde{\boldsymbol{\Delta}}_{\mathcal{S}_k}\boldsymbol{C}\boldsymbol{C}^H}(x) = 1 - \mathcal{F}(x,\beta)/4\beta x$ into (25), we have

$$1 - \frac{\mathcal{F}(x,\beta)}{4\beta x} = \eta_{\tilde{\boldsymbol{\Delta}}_{\mathcal{S}_k}}\left(x \frac{1 - \frac{\mathcal{F}(x,\beta)}{4\beta x} + \beta - 1}{1 - \frac{\mathcal{F}(x,\beta)}{4\beta x}} \right). \tag{49}$$

Using variable substitution and some regular but tedious manipulations, we can derive that

$$\eta_{\tilde{\boldsymbol{\Delta}}_{\mathcal{S}_k}}(x) = q(x) \tag{50}$$

where $q(x) \triangleq (\sqrt{4x+1} - 1)/(2x)$.

As a result, we can conclude that, in the relay system using the orthogonal spreading sequence, if in a channel $\eta_{\boldsymbol{\Delta}_{\mathcal{S}_k}}(x) < q(x)$, the system with local CSI at every node is superior to that with global CSI at the relay. Otherwise, the result is the opposite.

Take the Nakagami-m fading channel as an example, where $\eta_{\boldsymbol{\Delta}_{\mathcal{S}_k}}(x) = p(x,m)$. We plot $q(x)$ and compare it with $p(x,m)$ $\forall m \geq 1$ in Fig. 2, which shows that $p(x,m) \leq q(x)$ $\forall m \geq 1$. Therefore

$$\bar{\gamma}_{\mathrm{MAC}_k}^{L-\mathrm{Orth}} \geq \bar{\gamma}_{\mathrm{MAC}_k}^{G} \qquad \forall m \geq 1. \tag{51}$$

It indicates that, in Nakagami-m channels $(m \geq 1)$, the relay system with local CSI at every node is spectrally more efficient than the system with global CSI at the relay, when the orthogonal spreading sequence is employed.

C. Intuitive Interpretation

To understand why there is a performance difference between the relay systems with different CSI, we investigate the orthogonality of the equivalent channels in different S–R links, which is measured by correlation coefficients. A lower correlation coefficient indicates more orthogonal equivalent channels.

It is interesting to see that even when the two systems with different CSI using the same spreading sequence and undergoing the same fading channel, the correlation coefficients between the equivalent channels of different users in the two systems are not identical.

For the system with global CSI at the relay, each source employs its own spreading sequence for precoding, which does not depend on the channel information. From the view of the relay, the received signals from source $\mathcal{S}_i$ and $\mathcal{S}_k$ experience different channels, and their equivalent channels are $\boldsymbol{H}_{\mathcal{S}_i}\boldsymbol{c}_i$ and $\boldsymbol{H}_{\mathcal{S}_k}\boldsymbol{c}_k$, respectively. Both the spreading sequences and channel responses are different. The correlation coefficient between the equivalent channels from $\mathcal{S}_i$ and $\mathcal{S}_k$ seen at the relay is

$$\rho_{ik}^{G} = \frac{\left|\boldsymbol{c}_i^H \boldsymbol{H}_{\mathcal{S}_i}^H \boldsymbol{H}_{\mathcal{S}_k}\boldsymbol{c}_k\right|}{\|\boldsymbol{H}_{\mathcal{S}_i}\boldsymbol{c}_i\| \cdot \|\boldsymbol{H}_{\mathcal{S}_k}\boldsymbol{c}_k\|}. \tag{52}$$

For the system with local CSI at every node, each source can employ channel-dependent precoder while the relay receives signals with different spreading sequences for different users. Because source $\mathcal{S}_k$ only has its own channel information, it implicitly assumes that other sources have the same channel as itself when designing the Max-SLNR precoder, as shown in (18). That is to say, from the view of source $\mathcal{S}_k$, the equivalent channels of $\mathcal{S}_i$ and $\mathcal{S}_k$ are $\boldsymbol{H}_{\mathcal{S}_k}\boldsymbol{c}_i$ and $\boldsymbol{H}_{\mathcal{S}_k}\boldsymbol{c}_k$, respectively, where only the spreading sequences are different. Therefore, the correlation coefficient of the equivalent channels of $\mathcal{S}_i$ and $\mathcal{S}_k$ seen at the kth source becomes

$$\rho_{ik}^{L} = \frac{\left|\boldsymbol{c}_i^H \boldsymbol{H}_{\mathcal{S}_k}^H \boldsymbol{H}_{\mathcal{S}_k}\boldsymbol{c}_k\right|}{\|\boldsymbol{H}_{\mathcal{S}_k}\boldsymbol{c}_i\| \cdot \|\boldsymbol{H}_{\mathcal{S}_k}\boldsymbol{c}_k\|}. \tag{53}$$

By comparing (52) and (53), we can observe that the orthogonality of the equivalent channels seen at the relay depends on the cross correlation of different spreading sequences weighted by different channel power responses. By contrast, the orthogonality seen at each source relies on the cross correlation of

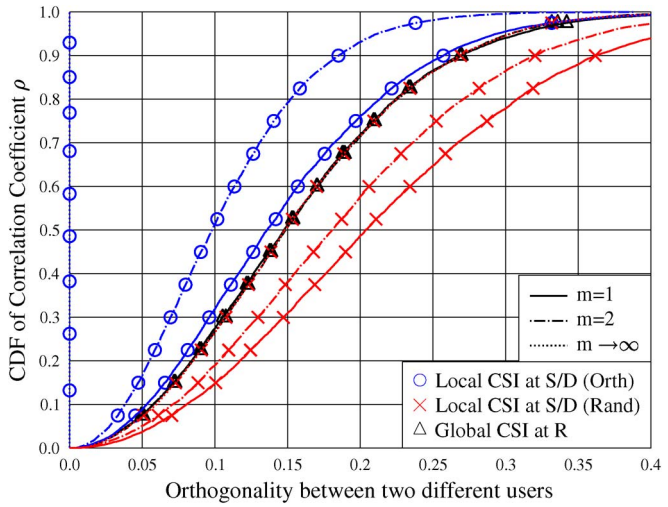

Fig. 3. CDF of correlation coefficients in Nakagami-m fading channels.

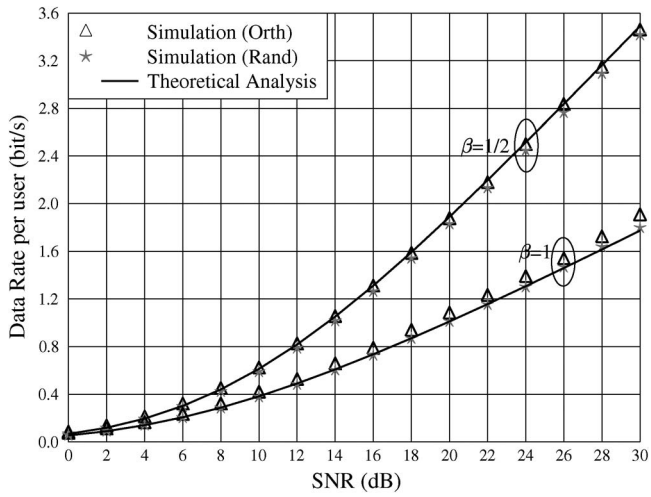

Fig. 4. Data rate per user of the AF relay system with global CSI at the relay versus SNR.

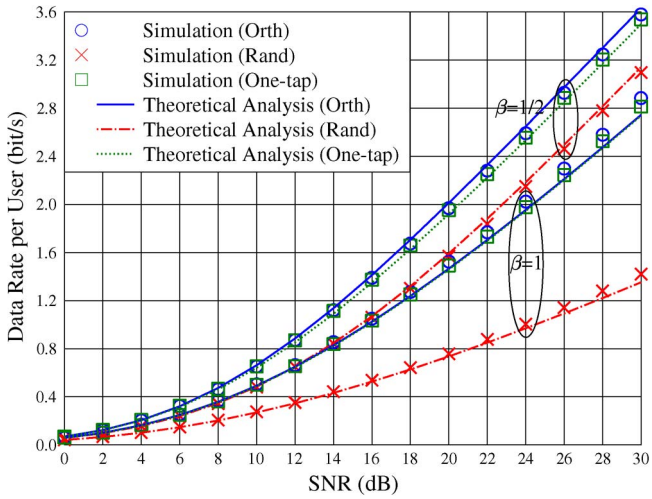

Fig. 5. Data rate per user of the AF relay system with local CSI at every node versus SNR.

different spreading sequences weighted by the same channel power responses.

In Fig. 3, we present the cumulative distribution function (cdf) of the correlation coefficients in Nakagami-m $(m \geq 1)$ fading channels. It is shown that the orthogonality of the equivalent channels seen at the relay is almost the same for different m, no matter if the spreading sequences are orthogonal or random. This explains why the asymptotic SINR of the system with global CSI at the relay is independent of the features of fading channels and spreading sequences. By contrast, the orthogonality of the equivalent channels seen at the source is sensitive to the spreading sequences and the channels. When the orthogonal spreading sequence is used, the orthogonality of the equivalent channels seen at the source is always better than that at the relay. However, when the random spreading sequence is employed, the orthogonality of the equivalent channels at the source becomes inferior to that at the relay. Moreover, in Nakagami-m fading channels, when m increases, the equivalent channels at the sources become more orthogonal, and their correlation coefficient approaches to the maximum value when $m \to \infty$.

Note that the performance of the linear transceiver largely depends on the orthogonality of equivalent channels. As a result, the system with local CSI at every node achieves higher spectral efficiency than the system with global CSI at the relay when the orthogonal spreading sequence is applied. However, the system with global CSI at the relay will become superior when the random spreading sequence is used.

VI. Simulation and Numerical Results

Here, we validate previous analysis by comparing the asymptotic spectral efficiency with the average spectral efficiency obtained through simulations with finite K and M. In the simulation, we consider that the noise at the relay and destination has the same variance of $\sigma_{\mathcal{R}}^2 = \sigma_{\mathcal{D}}^2 = \sigma^2$. We consider frequency-selective Rayleigh or Nakagami-m fading channels. The transmit power is equally allocated to each symbol at the source and the relay, i.e., $P_{\mathcal{S}} = P_{\mathcal{R}} = P/2$. The SNR per symbol is P/σ^2. In the legends, "Orth" means a system using the orthogonal spreading sequence, "Rand" denotes a system using the random spreading sequence, and "One-tap" stands for the constructed spreading sequence that yields the low-complexity transceiver.

We show the data rate per user versus SNR of the relay system with global CSI at the relay in Fig. 4 (with legend "Global CSI at R") and that with local CSI at every node (with legend "Local CSI at S/D") in Fig. 5. We also compare the numerical results obtained from the asymptotic analysis (with legend "Theoretical Analysis") and the simulation results for a relay system transmitted over $M = 32$ subcarriers in a fading channel with $L = 8$ resolvable paths (with legend "Simulation"). In Fig. 4, the analytical result is numerically obtained from (16), whereas in Fig. 5, the analytical results are numerically obtained from (27), (28), and (46), respectively. In the simulation, because $L < M$, the adjacent subcarriers are correlated, but the correlation among the adjacent subcarriers are not very strong in the considered setting.

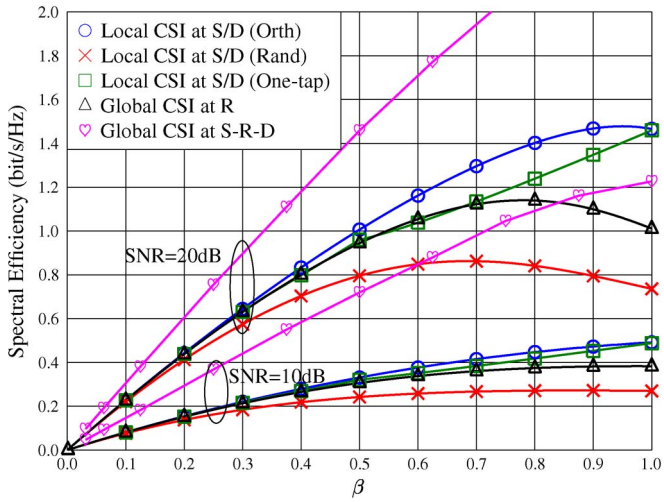

Fig. 6. Spectral efficiency comparison in Rayleigh fading channels with AF relays.

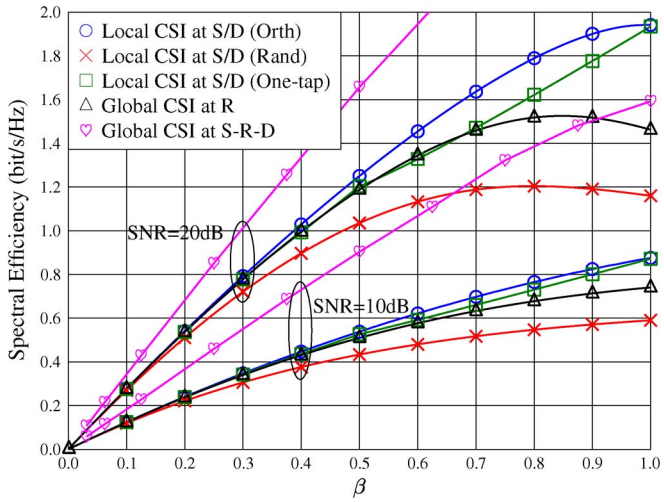

Fig. 7. Spectral efficiency comparison in Rayleigh fading channels with DF relays.

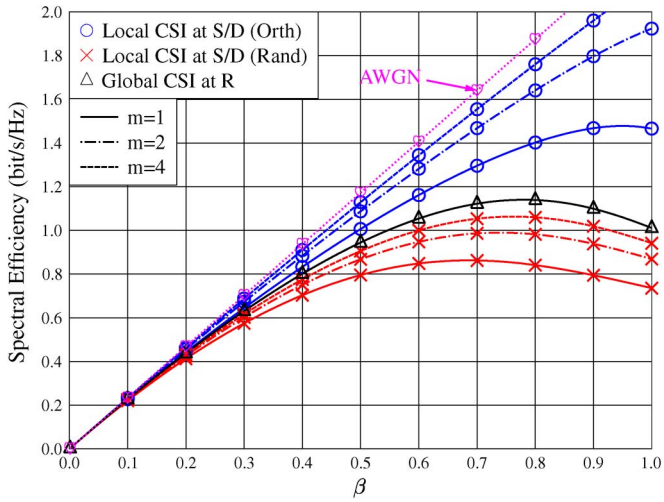

Fig. 8. Impact of fading channels on the spectral efficiency with AF relays.

It shows that the numerical results are close to the simulation results with finite numbers of users and subcarriers for arbitrary SNR. This indicates that the asymptotic spectral efficiency rapidly converges to the average spectral efficiency. This also shows that the approximations used in the derivation are accurate. Moreover, in the analysis, we assumed that the channel coefficients among subcarriers are mutually independent, but in the simulations, the channels between adjacent subcarriers are correlated. It implies that the conclusions drawn from the analytical analysis are also true for practical channels without the assumption. This is because the performance of the two systems with different CSI depends on the orthogonality among the equivalent channels, which are weighted by the spreading sequences. Different users employ different spreading sequences, which will randomize the equivalent channels. In Fig. 4, we see that when using the global CSI at the relay, the data rate per user is almost the same, regardless of if the spreading sequences are orthogonal or random. However, in Fig. 5, it is clear that the performance varies with different spreading sequences. Moreover, the orthogonal spreading sequence achieves the maximal spectral efficiency, whereas the random spreading sequence achieves the minimal one. Their performance gap increases with the asymptotic load factor. In addition, the performance of the one-tap spreading sequence is quite close to that of the orthogonal spreading sequence. This validates our previous analytical analysis.

In Figs. 6 and 7, we show the numerical results of the asymptotic spectral efficiency of the systems with AF and DF relays, respectively. We investigate the spectral efficiency with different CSI using different spreading sequences. With both AF and DF relays, for arbitrary β and SNR, when the orthogonal spreading sequence is used, the system with local CSI at every node is spectrally more efficient than that with global CSI at the relay. When the random spreading sequence is employed, the result is the opposite. To show the performance upper bound of the relay systems, we also provide the performance of a system with global CSI at all nodes and the relay (with legend "Global CSI at S–R–D"). Under such a channel assumption, a joint S–R–D transceiver optimization in [10] can be applied. As expected, the jointly optimized transceiver with global CSI at all nodes and the relay achieves the highest spectral efficiency. This however comes at a cost of the complexity to iteratively compute precoders and detectors and a cost of the overhead to gather the global CSI for all nodes and the relay. In the considered setting, the DF relay outperforms the AF relay. When using the orthogonal spreading sequence, from the result of SNR $= 20$ dB with AF relay, we can see that the maximal spectral efficiency of the system with local CSI at every node is 1.48 bit/s/Hz (at $\beta = 0.95$), whereas that with global CSI at the relay is 1.14 bit/s/Hz (at $\beta = 0.8$). Compared with the system with global CSI at the relay, the system with local CSI at every node can improve 30% of the spectral efficiency when the load factor increases by 20%. Moreover, as we have discussed, acquiring the local CSI at every node needs much less training overhead than acquiring the global CSI at the relay. This suggests that if we consider the net throughput excluding the overhead for channel acquisition, the relay system with local CSI and the orthogonal spreading sequence is highly desirable.

To illustrate the impact of channel statistics on the performance, in Fig. 8, we compare the numerical results of the asymptotic spectral efficiency of the relay systems in Nakagami-m fading channels with different m. The performance in the AWGN channel is also shown as a reference. When m increases, the performance of the system with global CSI at the relay almost does not change, whereas that with local CSI at every node becomes better. When considering the orthogonal spreading sequence, the spectral efficiency provided by the system with local CSI approaches that in the AWGN channel. When employing the random spreading sequence, the spectral efficiency provided by the system with local CSI at every node goes to that with global CSI at the relay.

All these results agree with our analytical analysis very well.

VII. Conclusion

In this paper, we have analyzed the spectral efficiency of MC-CDMA two-hop relay systems with different CSI: In one system, only the relay has global CSI, and in the other system, only each source and each destination node have local CSI. It is shown from both analytical and simulation results that the spectral efficiency of the system with global CSI at the relay is immune to the features of the spreading sequences and fading channel statistics. By contrast, the spectral efficiency of the system with local CSI at every node depends on these factors. In Nakagami-m fading channels, compared with the system with global CSI, the system with local CSI is spectrally more efficient when the spreading sequence is orthogonal but is less efficient when the spreading sequence is random. When the one-tap spreading sequence is applied, the system with local CSI at every node can significantly reduce the transceiver complexity of the source and destination nodes yet only suffers from minor performance loss. If we are accounting for the training overhead to facilitate channel estimation, the net throughput of the relay system with local CSI at every node will be much higher than that of the relay system with global CSI at the relay when the spreading sequence is properly designed.

Appendix A
Derivation of $\partial\bar{\gamma}^L_{\mathrm{MAC}_k}/\partial(P_{\mathcal{S}}/\sigma^2_{\mathcal{R}})$

Let $y=\bar{\gamma}^L_{\mathrm{MAC}_k}$ and $x=P_{\mathcal{S}}/\sigma^2_{\mathcal{R}}$; (29) can be rewritten as

$$\beta-1+\frac{\beta}{y+1}+\eta_{\mathbf{\Delta}_{\mathcal{S}_k}}\left(\frac{\beta x}{\phi y+1}\right)=0. \tag{54}$$

Apply the implicit differentiation to (54); we have

$$\frac{\beta}{(y+1)^2}\frac{\partial y}{\partial x}+\eta'_{\mathbf{\Delta}_{\mathcal{S}_k}}(z)\left(\frac{\beta}{\phi y+1}-\frac{\beta\phi x}{(\phi y+1)^2}\frac{\partial y}{\partial x}\right)=0 \tag{55}$$

where $z=\beta x/(\phi y+1)$, and $\eta'_{\mathbf{\Delta}_{\mathcal{S}_k}}(z)=\partial\eta_{\mathbf{\Delta}_{\mathcal{S}_k}}(z)/\partial z$ is the first-order derivative of $\eta_{\mathbf{\Delta}_{\mathcal{S}_k}}(z)$.

Then, (55) can further be rewritten as

$$\frac{\partial y}{\partial x}\left(\frac{1}{(y+1)^2}-\frac{\eta'_{\mathbf{\Delta}_{\mathcal{S}_k}}(z)\phi x}{(\phi y+1)^2}\right)=-\frac{\eta'_{\mathbf{\Delta}_{\mathcal{S}_k}}(z)}{\phi y+1} \tag{56}$$

i.e.,

$$\frac{\partial y}{\partial x}=\frac{-\eta'_{\mathbf{\Delta}_{\mathcal{S}_k}}(z)(\phi y+1)}{\frac{(\phi y+1)^2}{(y+1)^2}-\eta'_{\mathbf{\Delta}_{\mathcal{S}_k}}(z)\phi x}. \tag{57}$$

From (13), we obtain

$$\eta'_{\mathbf{\Delta}_{\mathcal{S}_k}}(z)=\frac{\partial\eta_{\mathbf{\Delta}_{\mathcal{S}_k}}(z)}{\partial z}=-\int\frac{tf_{\mathbf{\Delta}_{\mathcal{S}_k}}(t)}{(1+tz)^2}dt\le 0. \tag{58}$$

Since the values of ϕ, y, and $-\eta'_{\mathbf{\Delta}_{\mathcal{S}_k}}(z)$ are always positive for $\beta<1$, it is not difficult to show that $\partial y/\partial x>0$, i.e., $\partial\bar{\gamma}^L_{\mathrm{MAC}_k}/\partial(P_{\mathcal{S}}/\sigma^2_{\mathcal{R}})>0\ \forall\beta<1$.

Appendix B
Proof of Theorem 1

Suppose that if $\eta_{\mathbf{\Delta}_A}(x)\ge\eta_{\mathbf{\Delta}_B}(x)$, $\bar{\gamma}^L_A\ge\bar{\gamma}^L_B$.

When $\eta_{\mathbf{\Delta}_A}(x)\ge\eta_{\mathbf{\Delta}_B}(x)$, i.e., $1-\eta_{\mathbf{\Delta}_A}(x)\le 1-\eta_{\mathbf{\Delta}_B}(x)$, we have

$$1-\eta_{\mathbf{\Delta}_A}\left(\frac{P_{\mathcal{S}}}{\sigma^2_{\mathcal{R}}}\frac{\beta}{\phi\bar{\gamma}^L_A+1}\right)\le 1-\eta_{\mathbf{\Delta}_B}\left(\frac{P_{\mathcal{S}}}{\sigma^2_{\mathcal{R}}}\frac{\beta}{\phi\bar{\gamma}^L_A+1}\right). \tag{59}$$

When $\bar{\gamma}_A\ge\bar{\gamma}_B$, we have $1/(\phi\bar{\gamma}^L_A+1)\le 1/(\phi\bar{\gamma}^L_B+1)$. From (58), it is easy to show that $\partial(1-\eta_{\mathbf{\Delta}_B}(x))/\partial x\ge 0$, i.e., $1-\eta_{\mathbf{\Delta}_B}(x)$ is an increasing function of x. Hence, we obtain

$$1-\eta_{\mathbf{\Delta}_B}\left(\frac{P_{\mathcal{S}}}{\sigma^2_{\mathcal{R}}}\frac{\beta}{\phi\bar{\gamma}^L_A+1}\right)\le 1-\eta_{\mathbf{\Delta}_B}\left(\frac{P_{\mathcal{S}}}{\sigma^2_{\mathcal{R}}}\frac{\beta}{\phi\bar{\gamma}^L_B+1}\right). \tag{60}$$

From (59) and (60), we have

$$1-\eta_{\mathbf{\Delta}_A}\left(\frac{P_{\mathcal{S}}}{\sigma^2_{\mathcal{R}}}\frac{\beta}{\phi\bar{\gamma}^L_A+1}\right)\le 1-\eta_{\mathbf{\Delta}_B}\left(\frac{P_{\mathcal{S}}}{\sigma^2_{\mathcal{R}}}\frac{\beta}{\phi\bar{\gamma}^L_B+1}\right). \tag{61}$$

By substituting (61) into (29), the following inequality holds:

$$\frac{\bar{\gamma}^L_A}{\bar{\gamma}^L_A+1}\le\frac{\bar{\gamma}^L_B}{\bar{\gamma}^L_B+1}. \tag{62}$$

Then, we show that $\bar{\gamma}^L_A\le\bar{\gamma}^L_B$, which contradicts the assumption. Thus, the theorem is true.

Appendix C
Proof of Corollary 1

By substituting $\eta_{\mathbf{\Delta}_{\mathcal{S}_k}}=1/(1+x)$ into (27) and using some regular but tedious manipulations, we can show that the upper bound of $\bar{\gamma}^{L-\mathrm{Rand}}_{\mathrm{MAC}_k}$ is the solution of

$$x^2-\left((1-\beta)P_{\mathcal{S}}/\sigma^2_{\mathcal{R}}-1\right)x-P_{\mathcal{S}}/\sigma^2_{\mathcal{R}}=0. \tag{63}$$

Omitting one negative solution, the closed-form expression of the upper bound of $\bar{\gamma}^{L-\mathrm{Rand}}_{\mathrm{MAC}_k}$ is

$$\begin{aligned}x&=\frac{1}{2}\left((1-\beta)z-1+\sqrt{((1-\beta)z-1)^2+4z}\right)\\&=z-\frac{1}{2}\left((1+\beta)z+1-\sqrt{(1-\beta)^2z^2-(1+\beta)+1}\right)\end{aligned}$$

$$= z - \frac{1}{4}\left(1 + (1+\sqrt{\beta})^2 z + 1 + (1-\sqrt{\beta})^2 z\right) - \frac{1}{4}\left(2\sqrt{\left(1 + (1+\sqrt{\beta})^2 z\right)\left(1 + (1-\sqrt{\beta})^2 z\right)}\right)$$

$$= z - \frac{1}{4}\left(\sqrt{1 + (1+\sqrt{\beta})^2 z} - \sqrt{1 + (1-\sqrt{\beta})^2 z}\right)^2$$

$$= z - \frac{1}{4}\mathcal{F}(z, \beta). \tag{64}$$

where $z = P_{\mathcal{S}}/\sigma_{\mathcal{R}}^2$.

Therefore, (34) is the upper bound of $\bar{\gamma}_{\mathrm{MAC}_k}^{L-\mathrm{Rand}}$.

Similarly, substituting the η-transform into (28), we can show that the upper bound of $\bar{\gamma}_{\mathrm{MAC}_k}^{L-\mathrm{Orth}}$ is the solution of

$$(1-\beta)x^2 - \left((1-\beta)P_{\mathcal{S}}/\sigma_{\mathcal{R}}^2 - 1\right)x - P_{\mathcal{S}}/\sigma_{\mathcal{R}}^2 = 0. \tag{65}$$

Again, omitting the negative solution, we obtain

$$x = \frac{(1-\beta)z - 1 + \sqrt{\left((1-\beta)z - 1\right)^2 + 4z(1-\beta)}}{2(1-\beta)} = \frac{(1-\beta)z - 1 + (1-\beta)z + 1}{2(1-\beta)} = z. \tag{66}$$

Hence, (35) is the upper bound of $\bar{\gamma}_{\mathrm{MAC}_k}^{L-\mathrm{Orth}}$.

REFERENCES

[1] J. N. Laneman, D. N. C. Tse, and G. W. Wornell, "Cooperative diversity in wireless networks: Efficient protocols and outage behavior," *IEEE Trans. Inf. Theory*, vol. 50, no. 12, pp. 3062–3080, Dec. 2004.

[2] C. Esli and A. Wittneben, "One- and two-way decode-and-forward relaying for wireless multiuser MIMO networks," in *Proc. IEEE GLOBECOM*, Dec. 2008, pp. 1–6.

[3] M. Chen and A. Yener, "Power allocation for F/TDMA multiuser two-way relay networks," *IEEE Trans. Wireless Commun.*, vol. 9, no. 2, pp. 546–551, Feb. 2010.

[4] E. Yilmaz, R. Zakhour, D. Gesbert, and R. Knopp, "Multi-pair two-way relay channel with multiple antenna relay station," in *Proc. IEEE ICC*, May 2010, pp. 1–5.

[5] R. Zhang, C.-C. Chai, and Y.-C. Liang, "Joint beamforming and power control for multiantenna relay broadcast channel with QoS constraints," *IEEE Trans. Signal Process.*, vol. 57, no. 2, pp. 726–737, Feb. 2009.

[6] S. Berger, M. Kuhn, A. Wittneben, T. Unger, and A. Klein, "Recent advances in amplify-and-forward two-hop relaying," *IEEE Commun. Mag.*, vol. 47, no. 7, pp. 50–56, Jul. 2009.

[7] A. Osseiran, E. Hardouin, A. Gouraud, M. Boldi, I. Cosovic, K. Gosse, J. Luo, S. Redana, W. Mohr, J. Monserrat, T. Svensson, A. Tolli, A. Mihovska, and M. Werner, "The road to IMT-advanced communication systems: State-of-the- art and innovation areas addressed by the WINNER + project," *IEEE Commun. Mag.*, vol. 47, no. 6, pp. 38–47, Jun. 2009.

[8] C. Song, K.-J. Lee, and I. Lee, "MMSE based transceiver designs in closed-loop non-regenerative MIMO relaying systems," *IEEE Trans. Wireless Commun.*, vol. 9, no. 7, pp. 2310–2319, Jul. 2010.

[9] Y. Rong, X. Tang, and Y. Hua, "A unified framework for optimizing linear nonregenerative multicarrier MIMO relay communication systems," *IEEE Trans. Signal Process.*, vol. 57, no. 12, pp. 4837–4851, Dec. 2009.

[10] C. B. Chae, T. Tang, R. W. Heath, and S. Cho, "MIMO relaying with linear processing for multiuser transmission in fixed relay networks," *IEEE Trans. Signal Process.*, vol. 56, no. 2, pp. 727–738, Feb. 2008.

[11] I. Cosovic and S. Kaiser, "A unified analysis of diversity exploitation in multicarrier CDMA," *IEEE Trans. Veh. Technol.*, vol. 56, no. 4, pp. 2051–2062, Jul. 2007.

[12] T. Liu, L.-L. Yang, and C. Yang, "Spectral-efficiency of TDD multiuser two-hop MC-CDMA systems employing egocentric-altruistic relay optimization," in *Proc. IEEE VTC Spring*, May 2010, pp. 1–5.

[13] R. Krishna, Z. Xiong, and S. Lambotharan, "A cooperative MMSE relay strategy for wireless sensor networks," *IEEE Signal Process. Lett.*, vol. 15, pp. 549–552, 2008.

[14] R. Zhang, Y.-C. Liang, C.-C. Chai, and S. Cui, "Optimal beamforming for two-way multi-antenna relay channel with analogue network coding," *IEEE J. Sel. Areas Commun.*, vol. 27, no. 5, pp. 699–712, Jun. 2009.

[15] L.-L. Yang, "Joint transmitter-receiver design in TDD multiuser MIMO systems: An egocentric/altruistic optimization approach," in *Proc. IEEE VTC Spring*, Apr. 2007, pp. 2094–2098.

[16] S. Verdu and S. Shamai, "Spectral efficiency of CDMA with random spreading," *IEEE Trans. Inf. Theory*, vol. 45, no. 2, pp. 622–640, Mar. 1999.

[17] A. M. Tulino and S. Verdu, *Random Matrix Theory and Wireless Communications*. Hanover, MA: Now, 2004.

[18] J. G. Proakis, *Digital Communications*, 3rd ed. New York: McGraw-Hill, 1995.

[19] I. Gradshteyn and I. Ryzhik, *Table of Integrals, Series, and Products*, A. Jeffrey and D. Zwillinger, Eds., 7th ed. New York: Academic, 2007.

[20] M. K. Simon and M.-S. Alouini, *Digital Communication Over Fading Channels: A Unified Approach to Performance Analysis*. New York: Wiley, 2000.

[21] T. Liu and C. Yang, "A symbol-level FDE and spread-spectrum mode design for multi-code multiple access systems," in *Proc. IEEE ICC*, May 2008, pp. 4337–4341.

Tingting Liu (S'09–M'11) received the B.S. and Ph.D. degrees in signal and information processing from Beihang University, Beijing, China, in 2004 and 2011, respectively.

From December 2008 to January 2010, she was a Visiting Student with the School of Electronics and Computer Science, University of Southampton, Southampton, U.K. She is currently a Postdoctoral Fellow with the School of Electronics and Information Engineering, Beihang University. Her research interests include wireless communications and signal processing, multicarrier code-division multiple access, multiple-input–multiple-output, and distributed cooperative communications.

Chenyang Yang (SM'08) received the M.S.E and Ph.D. degrees in electrical engineering from Beihang University (formerly Beijing University of Aeronautics and Astronautics), Beijing, China, in 1989 and 1997, respectively.

She is currently a Full Professor with the School of Electronics and Information Engineering, Beihang University. She has published various papers and filed many patents in the fields of signal processing and wireless communications. Her recent research interests include signal processing in network multiple-input–multiple-output, cooperative communication, energy-efficient transmission, and interference management.

Prof. Yang is the Chair of the IEEE Communications Society Beijing Chapter. She has served as a Technical Program Committee Member for many IEEE conferences, such as the IEEE International Conference on Communications and the IEEE Global Telecommunications Conference. She currently serves as an Associate Editor for IEEE TRANSACTIONS ON WIRELESS COMMUNICATIONS, an Associate Editor-in-Chief of the *Chinese Journal of Communications*, and an Associate Editor-in-Chief of the *Chinese Journal of Signal Processing*. She was nominated as an Outstanding Young Professor of Beijing in 1995 and was supported by the First Teaching and Research Award Program for Outstanding Young Teachers of Higher Education Institutions by Ministry of Education (P. R. C. "TRAPOYT") during 1999 to 2004.